

YANJUN XIN^{1,2}, GANG WANG², YONGPING LIU³, ZHILIN ZANG², MENGCHUN GAO¹

EFFECT OF WO_3 ON THE MORPHOLOGY AND PHOTODEGRADATION OF DIMETHYL PHTHALATE OF TiO_2 NANOTUBE ARRAY PHOTOELECTRODE

WO_3 modified TiO_2 nanotube array (WO_3/TNA s) photoelectrodes were fabricated via electrochemical deposition on TNAs/Ti photoelectrodes. The morphology and structure of WO_3/TNA s photoelectrodes were investigated by scanning electron microscopy (SEM) and X-ray diffractometer (XRD). The effects of deposition potential, deposition duration, Na_2WO_4 concentration, and calcination temperature on the morphology and the photocatalytic activity were investigated. The results showed that suitable amounts of WO_3 promoted the photocatalytic activity of TNAs photoelectrodes for the degradation of dimethyl phthalate (DMP). The optimal conditions for the fabrication of WO_3/TNA s photoelectrodes were as follows: deposition voltage 3.0 V, 10 min deposition duration, 0.01 mol/dm³ Na_2WO_4 concentration, 1.5 cm electrode gap, and 550 °C annealing temperature. The degradation rate of DMP reached 77% after 60 min of illumination by WO_3/TNA s photoelectrode. Additionally, WO_3/TNA s photoelectrodes possessed superb stability for maintaining a high DMP degradation efficiency at more than 75% after 10 times of successive use with 60 min irradiation for each cycle. The enhancement of photocatalytic performance by the efficient combination of WO_3 with TNAs would provide a theoretical basis for the practical application of WO_3/TNA s photoelectrodes in water treatment.

1. INTRODUCTION

Phthalates (PAEs) are widely used as a plasticizers in industry. As one kind of PAEs, dimethyl phthalate (DMP) could accumulate in biological organisms and disturb the endocrine system even at a low concentration. DMP is a ubiquitous environmental pollutant and is listed as one of the priority pollutants by American EPA as well as by

¹The Key Laboratory of Marine Environmental Science and Ecology, Ministry of Education, Ocean University of China, Qingdao, 266003, China, corresponding author Y. Xin, e-mail address: xintom2000@126.com

²Qingdao Engineering Research Center for Rural Environment, College of Resource and Environment, Qingdao Agricultural University, Qingdao 266109, China.

³College of Science and Information, Qingdao Agricultural University, Qingdao 266109, China.

China's Ministry of Environmental Protection. Therefore, investigating methods for DMP degradation is critically important. Several such methods including photocatalytic oxidation [1–3], electrochemical degradation [4, 5], adsorption [6, 7] and sonoelectrolysis [8, 9] have been investigated.

In the last decade, TiO₂ nanotube arrays (TNAs) have received intense attention. They are considered one of the most promising photocatalysts for their remarkable ability of charge transport and superior oxidation [10–12]. However, TNAs photocatalysts, with band gap of 3.0–3.2 eV, could be activated only by UV radiation ($\lambda < 380$ nm) which accounts to less than 5% of solar energy on the Earth's surface [13].

To use the sunlight in an efficient way for TNAs photocatalyst, various doping materials have been used, such as C [14, 15], Pd [16], In [17], Bi [18], CdTe [19], CdS [20, 21], WO₃ [22] and Sb₂S₃ [23]. It is well known that WO₃ has a slightly lower conduction band (CB) than that of TiO₂, thus the photoelectrons could transfer from the CB of TiO₂ to the CB of WO₃ and the recombination of charge carriers is reduced [22].

In our previous study [24, 25], WO₃ was successfully incorporated onto TNAs surface by a convenient cycle pulse electrodeposition method in tungstate solution. In this research, the effects of deposition potential, the Na₂WO₄ concentration and the annealed temperature on the photodegradation of DMP were investigated.

2. EXPERIMENTAL

Chemicals and materials. Titanium foils (purity > 99.9%, 0.2 mm thick) were obtained from Baoji Titanium and Nickel Manufacture Limited Company, China. All chemicals were obtained as analytical reagent grade and used without further purification. The experimental solutions were prepared with doubly distilled water.

Sample preparation and characterization. The TNAs photoelectrode (20×10 mm) fabricated by our group [12] and platinum (Pt) sheet were separately used as a cathode and anode in 0.1 mol/dm³ Na₂SO₄ solution with various amounts of Na₂WO₄ (0.002, 0.005, 0.01, 0.03, 0.05 mol/dm³). The deposition process was conducted at various potentials (1, 3 and 5 V) and times (2–60 min). Then the samples were immediately rinsed with deionized water and dried at 378 K for 60 min. Finally the photoelectrodes were annealed at 400 °C, 550 °C, 600 °C and 700 °C each for 120 min. The surface morphology of fabricated photoelectrodes was studied by SEM (America QUANTA200F). The crystal structure was examined using X-ray diffractometer (XRD, Rigaku D/max-rb) with CuK_α radiation ($\lambda = 1.5418$) at 0.02° intervals of 2θ over the range of 10–90°.

Photocatalytic activity. The photocatalytic performance of WO₃/TNAs photoelectrode was investigated using DMP aqueous solution (40 cm³) in a single-compartment cylindrical quartz reactor. The concentration of DMP was 20 mg/dm³. Before photoreaction,

the sample solution was stirred in the dark for 30 min to reach adsorption/desorption equilibrium, then the sample solution, under magnetic stirring, was illuminated. A 75 W xenon lamp of was used as an external light source with the light intensity of 30.5 mW/cm² which would last 60 min. The DMP solution was collected at specific time intervals and analyzed immediately. The concentration of DMP was determined by the high performance liquid chromatography (HPLC, LC-20A, Shimadzu, Japan) with Inertsil ODS-SP column (150×4.6 mm, 5 μm). The detection optical wavelength was 228 nm. The mobile phase was mixture of methanol with water (9:1) with the flow rate of 1.0 cm³/min. The column temperature was 30 °C.

The degradation rate of DMP was calculated using the following formula:

$$D = \frac{C_0 - C}{C_0} \times 100\% \quad (1)$$

where C_0 is the initial concentration, C is the concentration after a certain period of illumination.

3. RESULTS AND DISCUSSIONS

3.1. MORPHOLOGY AND CRYSTAL STRUCTURE

Figure 1 shows the morphology of WO_3 /TNAs photoelectrodes fabricated at various deposition potentials in 0.01 mol/dm³ Na_2WO_4 and 0.1 mol/dm³ Na_2SO_4 .

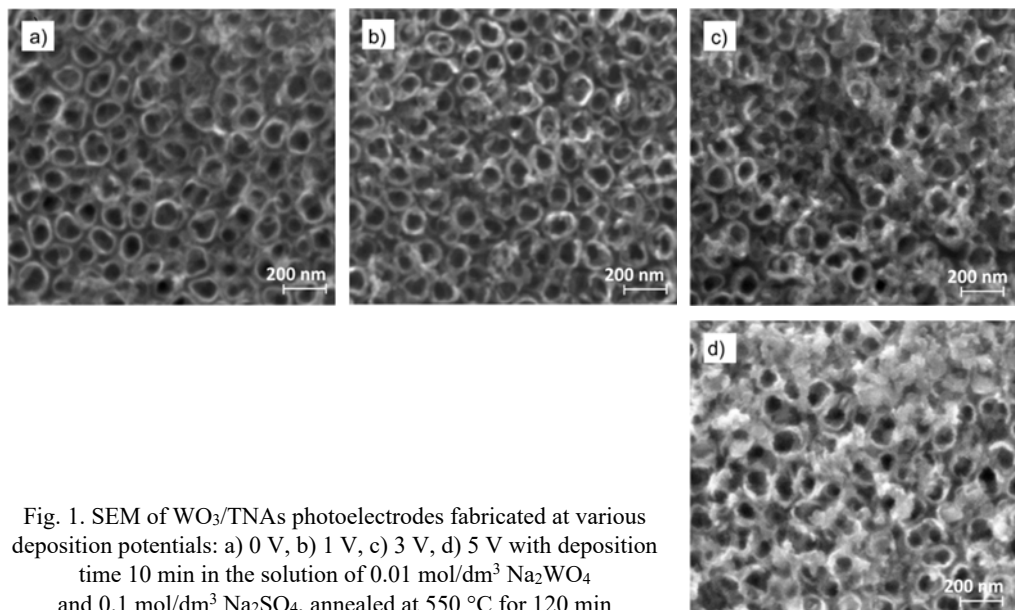


Fig. 1. SEM of WO_3 /TNAs photoelectrodes fabricated at various deposition potentials: a) 0 V, b) 1 V, c) 3 V, d) 5 V with deposition time 10 min in the solution of 0.01 mol/dm³ Na_2WO_4 and 0.1 mol/dm³ Na_2SO_4 , annealed at 550 °C for 120 min

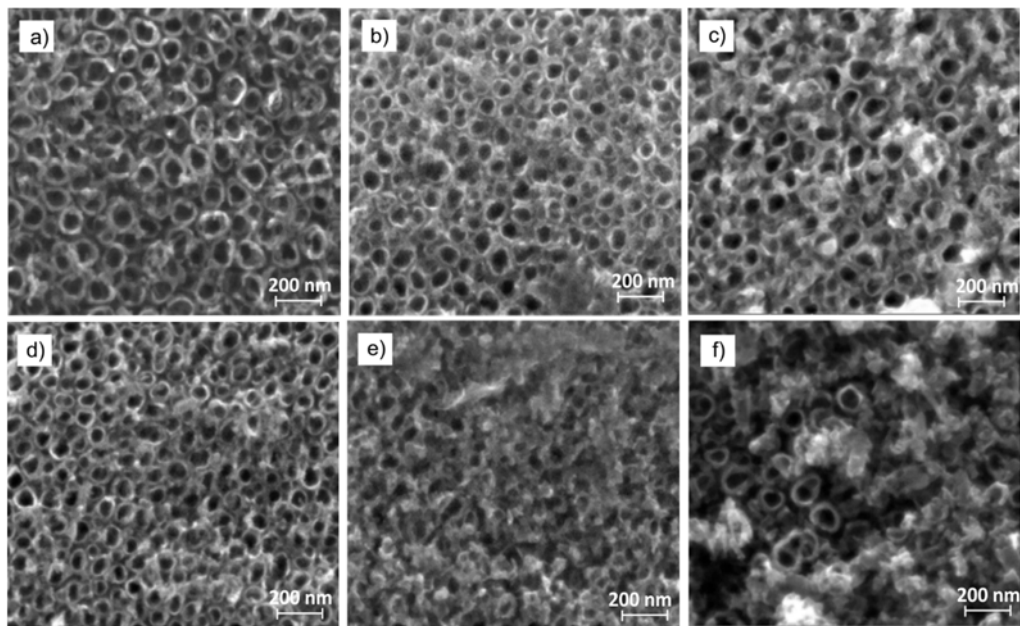


Fig. 2. SEM of WO_3/TNAs photoelectrodes fabricated at various Na_2WO_4 concentrations:
a) 0, b) 0.002 mol/dm³, c) 0.005 mol/dm³, d) 0.01 mol/dm³, e) 0.03 mol/dm³, f) 0.05 mol/dm³
with the deposition time 10 min, deposition potential 3 V, annealed at 550 °C for 120 min

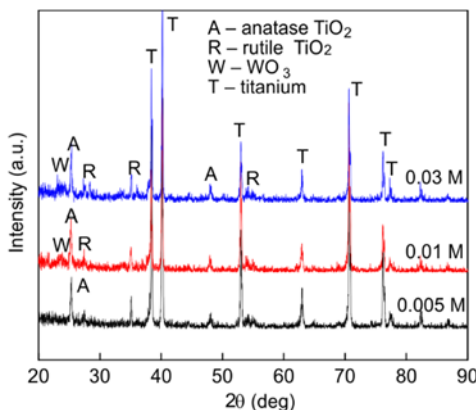


Fig. 3. XRD of WO_3/TNAs photoelectrodes
fabricated at various Na_2WO_4 concentrations
with the deposition time 10 min, deposition
potential 3 V, annealed at 550 °C for 120 min

The results showed that all WO_3/TNAs photoelectrodes have ordered nanotube arrays with the tube diameter of 90–100 nm and the wall thickness of 13–15 nm. There was no obvious difference between the photoelectrodes fabricated at 0 V and 1 V (Figs. 1a and 1b). However, the sediment was clearly present on the top of nanotube arrays when the deposition potential was 3 V (Fig. 1c). When the deposition potential was 5 V (Fig. 1d), some tubes were blocked. The results in Fig. 1 indicate that as the

deposition potentials increased, the sediment gradually increased as well. The morphology of $WO_3/TNAs$ photoelectrode fabricated at various Na_2WO_4 concentrations is shown in Fig. 2. The crystal structure of $WO_3/TNAs$ photoelectrode annealed at 550 °C for 120 min is shown in Fig. 3.

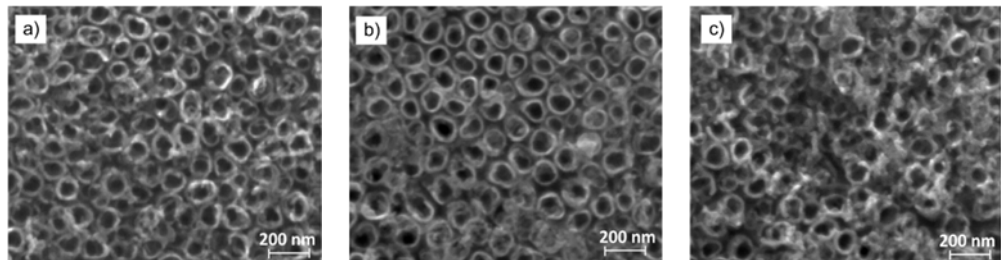


Fig. 4. SEM of $WO_3/TNAs$ photoelectrodes fabricated at various deposition times:
a) 0 min, b) 5 min, c) 10 min,
d) 20 min, e) 60 min
with the deposition potential 3 V,

Na_2WO_4 concentration
of 0.01 mol/dm³, annealed
at 550 °C for 120 min

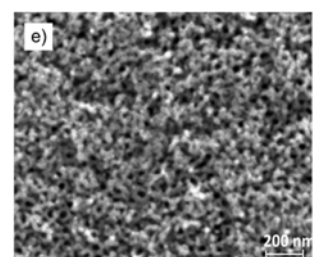
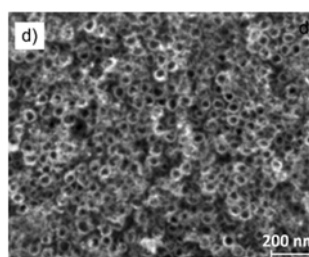
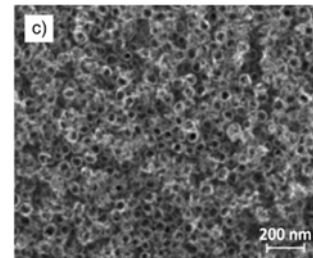
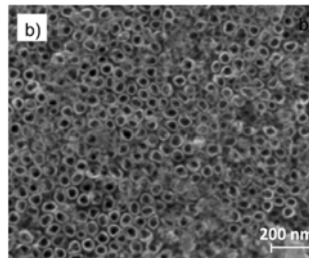
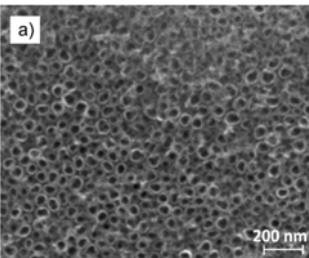
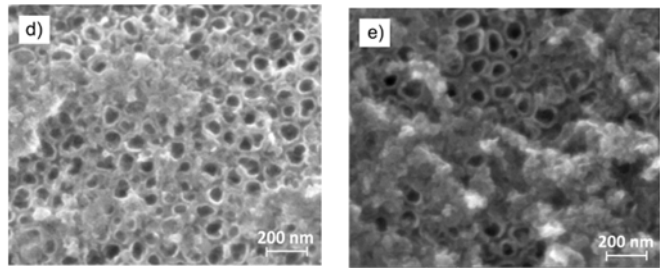


Fig. 5. SEM of $WO_3/TNAs$ photoelectrodes fabricated at various annealing temperatures: a) unannealed, b) 400 °C, c) 550 °C, d) 600 °C, e) 700 °C with the deposition potential 3 V, deposition time 10 min, and Na_2WO_4 concentration 0.01 mol/dm³

The results show that with an increasing concentration of Na_2WO_4 , the sediment on the top of nanotube array gradually increased (Figs. 2a–d). When the concentration

of Na_2WO_4 was $0.03 \text{ mol}/\text{dm}^3$, some nanotubes were blocked (Fig. 2e). A thick sediment covered the surface of nanotube array when the concentration of Na_2WO_4 increased to $0.05 \text{ mol}/\text{dm}^3$ (Fig. 2f). In Figure 3, a characteristic peak of WO_3 was found at 23.5° when the concentration of Na_2WO_4 increased from 0.01 to $0.03 \text{ mol}/\text{dm}^3$ which indicated that WO_3 was incorporated successfully onto TNAs. When the concentration of Na_2WO_4 was low at $0.002 \text{ mol}/\text{dm}^3$, WO_3 was not detected. As the Na_2WO_4 concentration increased, the amounts of WO_3 incorporated onto TNAs increased as well.

The morphology of WO_3/TNA s photoelectrodes annealed at various temperatures is shown in Fig. 5. The morphology of WO_3/TNA s photoelectrode annealed at 400°C showed no difference with that of unannealed photoelectrodes (Figs. 5a–b, respectively). When the photoelectrode was annealed at 550°C or 600°C , some fine particles emerged on the surface (Figs. 5c–d) for the aggregation of WO_3 . When the annealed temperature was 700°C , the nanotube collapsed and turned to worm state (Fig. 5e).

3.2. PHOTOCATALYTIC PERFORMANCE

The photodegradation rates of WO_3/TNA s photoelectrodes fabricated at various deposition potentials are shown in Fig. 6. When the deposition potential was lower than 3.0 V , upon its increase the photodegradation rate of DMP increased too and reached the peak of 82.6% . The degradation rate of DMP decreased when the potential exceeded 3.0 V .

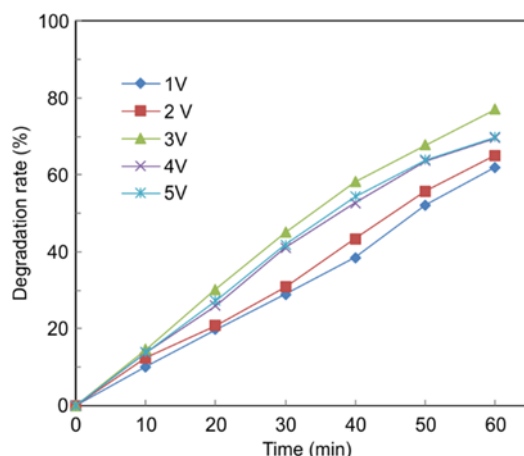


Fig. 6. Time dependences of the evolution of DMP photodegradation rate for WO_3/TNA s photoelectrodes fabricated at various deposition potentials; deposition time 10 min, Na_2WO_4 concentration $0.01 \text{ mol}/\text{dm}^3$, initial DMP concentration $20 \text{ mg}/\text{dm}^3$, and annealing temperature 550°C

The amount of WO_3 sediment on the surface of TNAs increased gradually with the increase of the deposition potential (Fig. 1). Compared with TNAs, WO_3 could absorb much more light and would trap the photogenerated electrons. Thus, the light quantum

efficiency was enhanced. However, too much WO_3 would block the mouth of nanotubes (Fig. 1) and therefore inhibited the light adsorption and the transfer of photogenerated electrons of TNAs, leading to a decreased rate of DMP photodegradation. The results verified that suitable amounts of WO_3 were beneficial to the photocatalytic activity of TNAs photoelectrode.

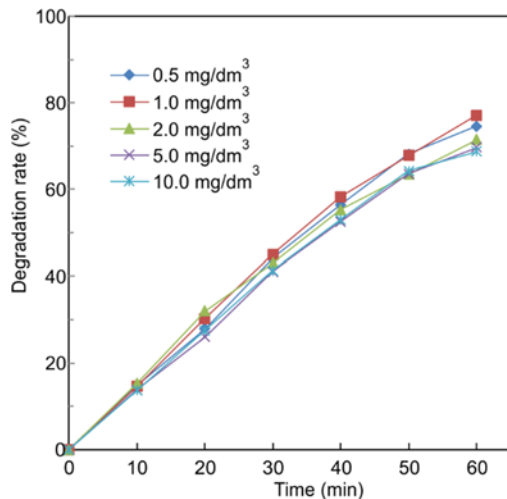


Fig. 7. Time dependences of the DMP photodegradation rate for WO_3 /TNAs photoelectrodes fabricated at various concentrations of Na_2WO_4 , deposition time 10 min, deposition potential 3 V, annealing temperature of 550 °C, initial DMP concentration 20 mg/dm^3

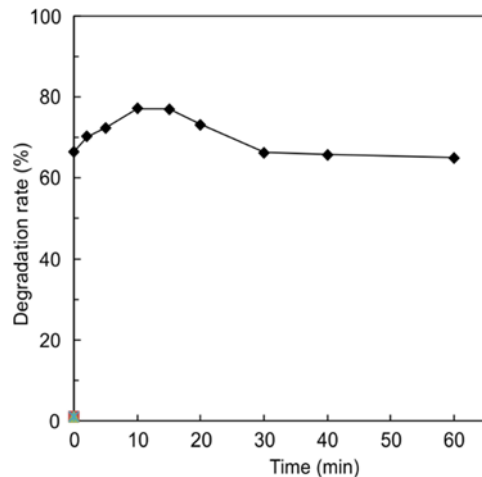


Fig. 8. Time dependences of the DMP photodegradation rate for WO_3 /TNAs photoelectrodes fabricated at Na_2WO_4 concentration of 0.01 mol/dm^3 , deposition potential 3 V, annealing temperature 550 °C, initial DMP concentration 20 mg/dm^3

Figure 7 presents the photodegradation rates of DMP for WO_3 /TNAs photoelectrodes fabricated at various Na_2WO_4 concentrations. The degradation rate of DMP increased when the concentration of Na_2WO_4 increased at the range of 0–0.01 mol/dm^3 . The photodegradation rate decreased when the concentration of Na_2WO_4 exceeded 0.01 mol/dm^3 . This agreed with previous experiments (Fig. 6) which showed that redundant WO_3 became the recombination centers of photogenerated electron-hole pairs and inhibited the light absorption of TNAs. Therefore, superfluous WO_3 would undermine the photodegradation rate of DMP for WO_3 /TNAs photoelectrode.

Figure 8 shows the photodegradation rates of DMP for WO_3 /TNAs photoelectrodes fabricated at various deposition times. The results indicated that the photodegradation rates of DMP increased with the deposition time when the time was shorter than 10 min. When the deposition time was over 15 min, the photodegradation rate of DMP decreased. This could be attributed to the excessive WO_3 sediment on the surface of TNAs

(Fig. 4), which inhibited the light absorption and the transfer of photogenerated carriers. The results were similar to those presented in Figs. 6 and 7.

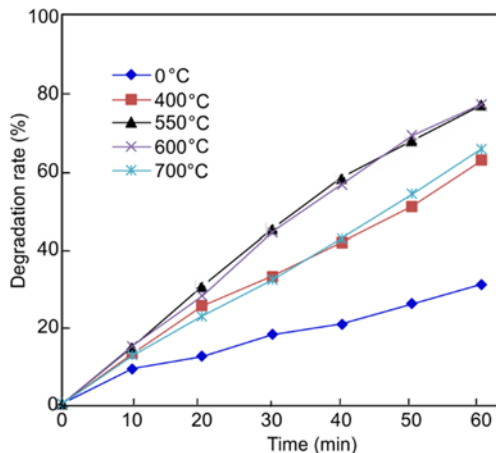


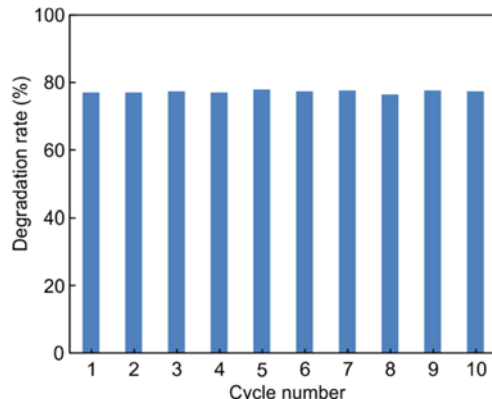
Fig. 9. Time dependences of the DMP photodegradation rate for WO_3/TNA s photoelectrodes fabricated at various annealing temperatures at Na_2WO_4 concentration of $0.01 \text{ mol}/\text{dm}^3$, deposition time 10 min, deposition potential 3 V. The initial DMP concentration was $20 \text{ mg}/\text{dm}^3$

The photodegradation rates of DMP for WO_3/TNA s photoelectrodes fabricated at various annealing temperatures are shown in Fig. 9. WO_3/TNA s photoelectrode without calcination displayed the lowest photodegradation rate of DMP after 60 min of illumination. The photodegradation rates of DMP for WO_3/TNA s photoelectrodes annealed at 400, 550, 600, and 700 °C reached 62.7, 77.1, 77.2 and 65.7%, respectively. The results verified that the WO_3/TNA s photoelectrode annealed at 550 and 600 °C performed excellent photocatalytic activity. The optimum photocatalytic performance was ascribed to the mixed crystal effect, which promoted the separation of photogenerated carriers [12, 26]. When the annealing temperature was 700 °C, the photodegradation rate of DMP decreased due to the collapse of nanotube array (Fig. 5e). The decrease caused the reduction of the specific surface area and was detrimental to the transfer of photogenerated electrons.

3.3. PHOTOCATALYTIC STABILITY OF WO_3/TNA S PHOTOELECTRODES

The stability of WO_3/TNA s photoelectrode is a significant indicator for evaluation of its practical application. In order to evaluate the stability of WO_3/TNA s photoelectrode, the degradation efficiency of DMP was investigated by recycling the photoelectrodes for 10 cycles under irradiation for 60 min in each cycle. The stability and reusability of the WO_3/TNA s photoelectrodes is shown in Fig. 10. The removal efficiency of DMP was above 76% for all cycles. The experimental results indicated excellent chemical stability of WO_3/TNA s photoelectrodes, which could be ascribed to the formation of a robust coupling structure between WO_3 and the TNAs.

Fig. 10. The evolution of DMP photodegradation rate with the photodegradation cycles for $WO_3/TNAs$ photoelectrodes fabricated at Na_2WO_4 concentration of $0.01\text{ mol}/dm^3$, deposition time 10 min, deposition potential 3 V, annealing temperature $550\text{ }^\circ C$, initial DMP concentration $20\text{ mg}/dm^3$, and 60 min illumination time for each cycle



4. CONCLUSIONS

Various $WO_3/TNAs$ photoelectrodes were fabricated by the electrodeposition method on TNAs substrate. The results showed that suitable amount of WO_3 could improve the photocatalytic activity of TNAs photoelectrode. Under the 3.0 V deposition potential, 10 min deposition time, $0.01\text{ mol}/dm^3$ Na_2WO_4 , and $550\text{ }^\circ C$ annealing temperature, the optimum photocatalytic performance of $WO_3/TNAs$ photoelectrode was achieved and the photodegradation rate of DMP reached 77% after 60 min of illumination. After re-using the WO_3/TNA photoelectrodes 10 times, the photodegradation rate was still over 76%. The enhancement of photocatalytic performance by incorporating WO_3 onto TNAs would provide a theoretical basis for the practical application of WO_3/TNA photoelectrodes in water treatment.

ACKNOWLEDGEMENTS

This work is supported by National Natural Science Foundation of China (No. 51208274, 51478490), China Postdoctoral Science Foundation (No. 2013M531651), and Natural Science Foundation of Shandong Province (No. ZR2012EEQ010, ZR. 2011EL044).

REFERENCES

- [1] HUNG C.H., YUAN C., LI H.W., *Photodegradation of diethyl phthalate with PANi/CNT/TiO₂ immobilized on glass plate irradiated with visible light and simulated sunlight-effect of synthesized method and pH*, J. Hazard. Mater., 2017, 322, 243.
- [2] CHANG C.F., MAN C.Y., *Magnetic photocatalysts of copper phthalocyanine-sensitized titania for the photodegradation of dimethyl phthalate under visible light*, Colloid. Surf. A, 2014, 441, 255.
- [3] CUI H., LIANG Z., ZHANG J.Z., LIU H., SHI J., *Enhancement of photocatalytic activity of TiO₂/carbon aerogel based on hydrophilic secondary pore structure*, RSC Adv., 2016, 6 (72), 68416.

- [4] WANG Y., LIU Y., LIU T., SONG S., GUI X., LIU H., TSIAKARAS P., *Dimethyl phthalate degradation at novel and efficient electro-Fenton cathode*, Appl. Catal. B: Environ., 2014, 156–157, 1.
- [5] SOUZA F.D., SAEZ C., CANIZARES P., MOTHEO A.D., RODRIGO M., *Electrochemical removal of dimethyl phthalate with diamond anodes*, J. Chem. Technol. Biotechnol., 2014, 89 (2), 282.
- [6] WANG J., WANG F., YAO J., WANG R., YUAN H., MASAKORALA K., CHOI M.M.F., *Adsorption and desorption of dimethyl phthalate on carbon nanotubes in aqueous copper(II) solution*, Colloid. Surf. A, 2013, 417, 47.
- [7] XU Z., CHENG L., SHI J., LU J., ZHANG W., ZHAO Y., LI F., CHEN M., *Kinetic study of the removal of dimethyl phthalate from an aqueous solution using an anion exchange resin*, Environ. Sci. Poll. Res., 2014, 21 (10), 6571.
- [8] XU L.J., CHU W., GRAHAM N., *A systematic study of the degradation of dimethyl phthalate using a high-frequency ultrasonic process*, Ultrason. Sonochem., 2013, 20 (3), 892.
- [9] SOUZA F.L., SAEZ C., CANIZARES P., MOTHEO A. J., RODRIGO M.A., *Sonoelectrolysis of wastewaters polluted with dimethyl phthalate*, Ind. Eng. Chem. Res., 2013, 52 (28), 9674.
- [10] ZHENG L., HAN S., LIU H., YU P., FANG X., *Hierarchical MoS₂ nanosheet@TiO₂ nanotube array composites with enhanced photocatalytic and photocurrent performances*, Small, 2016, 12 (11), 1527.
- [11] ESKANDARLOO H., HASHEMPOUR M., VICENZO A., FRANZ S., BADIEI A., BEHNAJADY M.A., BESTETTI M., *High-temperature stable anatase-type TiO₂ nanotube arrays. A study of the structure–activity relationship*, Appl. Catal. B: Environ., 2016, 185, 119.
- [12] XIN Y.J., LIU H.L., HAN L., ZHOU Y.B., *Comparative study of photocatalytic and photoelectrocatalytic properties of alachlor using different morphology TiO₂/Ti photoelectrodes*, J. Hazard. Mater., 2011, 192 (3), 1812.
- [13] CAI J., HUANG J., GE M., IOCZZIA J., LIN Z.Q., ZHANG K.Q., LAI Y.K., *Immobilization of Pt nanoparticles via rapid and reusable electropolymerization of dopamine on TiO₂ nanotube arrays for reversible SERS substrates and nonenzymatic glucose sensors*, Small, 2017, 13 (19), 1604240.
- [14] JANUS M., MARKOWSKA-SZCZUPAK A., KUSIAK-NEJMAN E., MORAWSKI A.W., *Disinfection of *E. coli* by carbon modified TiO₂ photocatalysts*, Environ. Prot. Eng., 2012, 38 (2), 89.
- [15] SUN M., MA X., CHEN X., SUN Y., CUI X., LIN Y., *A nanocomposite of carbon quantum dots and TiO₂ nanotube arrays: enhancing photoelectrochemical and photocatalytic properties*, RSC Adv., 2014, 4 (3), 1120.
- [16] CHENG X.W., LIU H.L., CHEN Q.H., LI J.J., WANG P., *Preparation and characterization of palladium nano-crystallite decorated TiO₂ nano-tubes photoelectrode and its enhanced photocatalytic efficiency for degradation of diclofenac*, J. Hazard. Mater., 2013, 254, 141.
- [17] WANG Q., QIAO J., ZHOU J., GAO S., *Fabrication of CuInSe₂ quantum dots sensitized TiO₂ nanotube arrays for enhancing visible light photoelectrochemical performance*, Electrochim. Acta, 2015, 167, 470.
- [18] ZHONG J.S., WANG Q.Y., ZHU X., CHEN D.Q., JI Z.G., *Solvothermal synthesis of flower-like Cu₃Bi₂S₃ sensitized TiO₂ nanotube arrays for enhancing photoelectrochemical performance*, J. Alloys Comp., 2015, 641, 144.
- [19] FENG H., TRAN.T.T., CHEN L., YUAN L., CAI Q., *Visible light-induced efficiently oxidative decomposition of p-Nitrophenol by CdTe/TiO₂ nanotube arrays*, Chem. Eng. J., 2013, 215, 591.
- [20] GAKHAR R., SMITH Y.R., MISRA M., CHIDAMBARAM D., *Photoelectric performance of TiO₂ nanotube array photoelectrodes sensitized with CdS 0.54 Se 0.46 quantum dots*, Appl. Surf. Sci., 2015, 355, 1279.
- [21] LU N., SU Y., LI J., YU H., QUAN X., *Fabrication of quantum-sized CdS-coated TiO₂ nanotube array with efficient photoelectrochemical performance using modified successive ionic layer absorption and reaction (SILAR) method*, Sci. Bull., 2015, 60 (14), 1281.

- [22] MOMENI M.M., GHAYEB Y., DAVARZADEH M., *WO₃ nanoparticles anchored on titania nanotube films as efficient photoanodes*, Surf. Eng., 2015, 31, (4), 259.
- [23] XIE H., QUE W., HE Z., ZHONG P., LIAO Y., WANG G., *Preparation and photocatalytic activities of Sb₂S₃/TiO₂ nanotube coaxial heterogeneous structure arrays via an ion exchange adsorption method*, J. Alloys Comp., 2013, 550, 314.
- [24] XIN Y., LIU H., LIU Y., MA D.D., CHEN Q., *Composition and photoelectrochemical properties of WO₃/TNAs photoelectrodes fabricated by in situ electrochemical method*, Electrochim. Acta, 2013, 104 (8), 308.
- [25] WANG G., CHEN Q., XIN Y., LIU Y., ZANG Z., HU C., ZHANG B., *Construction of graphene-WO₃/TiO₂ nanotube array photoelectrodes and its enhanced performance for photocatalytic degradation of dimethyl phthalate*, Electrochim. Acta, 2016, 222, 1903
- [26] BEHNAJADY M.A., ALAMDARI M. E., MODIRSHAHLA N., *Investigation of the effect of heat treatment process on characteristics and photocatalytic activity of TiO₂-UV100 nanoparticles*, Environ. Prot. Eng., 2013, 39 (1), 33.